Research Article | Vol. 30, No. 2 / 17 Jan 2022 / Optics Express 2503

Optics EXPRESS

Holographic curved waveguide combiner for HUD/AR with 1-D pupil expansion

CRAIG T. DRAPER AND PIERRE-ALEXANDRE BLANCHE*

College of Optical Sciences, The University of Arizona, 1630 E University Blvd, Tucson, AZ 85721, USA
**pablanche@optics.arizona.edu*

Abstract: We are presenting the optical ray tracing as well as an experimental prototype of a curved waveguide combiner with pupil expansion for augmented reality (AR) and mixed reality (MR) glasses. The curved waveguide combiner takes advantage of holographic optical elements both for injection and extraction of the image to correct the aberrations introduced during the propagation of light inside the waveguide. The holographic curved combiner presented has a cylindrical outer radius of curvature of 171.45 mm with a field of view of 13° (H) × 16° (V) at a viewing distance of 1 cm with a 5 × horizontal 1 dimension pupil expansion for an eyebox of 6.2 mm × 42.7 mm.

1. Introduction

Holographic waveguides for augmented reality (AR) and mixed reality (MR) glasses have shown significant advantages compared to other types of combiners. This is because the waveguide approach can, thanks to pupil replication, increase the eye box without compromising the field of view (FOV). However, holographic waveguides have so far been limited to flat substrates, that could be difficult to implement in some systems and lack aesthetic appeal. To the best of our knowledge, implementation of pupil replication has always used flat waveguides combiners. In this article, we are presenting for the first time the use of a curve waveguide which aberrations are corrected by holographic optical elements.

Near to eye display (NED) combiners need to be lightweight, have a small footprint, large FOV and easily integrated for social acceptability [1,2]. Some examples of combiners include semitransparent mirrors, dichroic mirrors, and holograms. A semitransparent mirror as a combiner generally suffers from small FOV since the last optical component is far from the viewer. On the other hand, a combiner based on holographic optical elements (HOEs) can act as the last element and potentially have a larger FOV making them an excellent candidate for head up display (HUD) and AR systems.

HOEs can be fabricated to diffract light which satisfies both its angular and wavelength requirements. They can appear clear with little ghosting effects and propagate out of view images into the eye making them excellent candidates for see through displays. Their ability to condense complicated optical systems into a thin hologram layer can lead to lightweight and small footprint systems.

In NED systems, the encompassed volume or footprint is an important property to manage. The footprint may include the projection optics and the combiner system. The projection optics create the FOV and pupil of a system. Using a pupil replicating combiner, a small projection system can be used leading to an overall smaller system footprint [3,4]. The advantage of pupil replication is that it decouples the eyebox size from the field of view [5]. This allows for the use of small form factor projection optics as an input source to the display. Pupil replication through HOEs on a waveguide involve an insertion hologram (H_{in}) which propagates light at total internal reflection (TIR) conditions to reach an extraction hologram (H_{out}) which outcouples a portion of the light when the rest is recirculated many times to replicate the input pupil. It has to be noted that, as long as the extracted beams are collimated, the image is not duplicated but it is the pupil

#445091 https://doi.org/10.1364/OE.445091
Journal © 2022 Received 26 Oct 2021; revised 30 Dec 2021; accepted 31 Dec 2021; published 11 Jan 2022

Optics EXPRESS

of the system that is extended. In this case, the viewer experience a single image that can be seen from an extended eyebox. [4]

Recently, pupil replication using waveguide combiner have been implemented with different optical elements such as: curve reflector combiner, micro-prisms combiner, polarizing diffractive elements (Pancharatnam–Berry gratings), cascaded half-mirrors, as well as free-form optics [1,6–8]. The advantage of HOEs over other techniques for AR and HUD applications is that these elements are thin, light, can cover a large surface (windshield), and can be mass produced using roll to roll technique. In addition, for the present study, HOEs have the advantage that they can easily be applied to curve surfaces.

Pupil replication has traditionally been limited to flat waveguides. However, flat waveguides have poor integration into spaces and lack aesthetic appeal. These may be reasons for the lack of public interest in currently available AR systems. The benefits of a curved waveguide display are its ease of integration and better conformity to the public's social standards. An example for AR would be if a person would rather wear a pair of glasses with flat substrates or if they would wear an aggressive looking device with curved substrates such as sunglasses. Another benefit may be larger possible FOV achievable as the waveguide wraps around the user [9]. In the case of HUD, a curved waveguide can also be integrated directly into a curved windshield instead of a separate waveguide system standing in front of it.

As of this moment, there is no information on pupil replicating curved waveguide combiners. Many have been limited to either a single exit pupil or expanding the pupil in the non-curved direction through a cylindrically curved waveguide such as the work done by Luminit [6].

2. System Design

The curved combiner consists of a cylindrically curved waveguide, an insertion HOE, and an extraction HOE. The HOEs are placed directly onto the waveguide and allow for coupling and extraction of light over an expanded pupil to act as a combiner display. A schematic of the light propagation in a curved waveguide is presented in Fig. 1, where we can see that, if no correction is applied, the incident beam will be reshaped by the refraction induced by the curved surface of the waveguide during injection, and by the multiple TIR reflections on the curved surface of the waveguide during propagation.

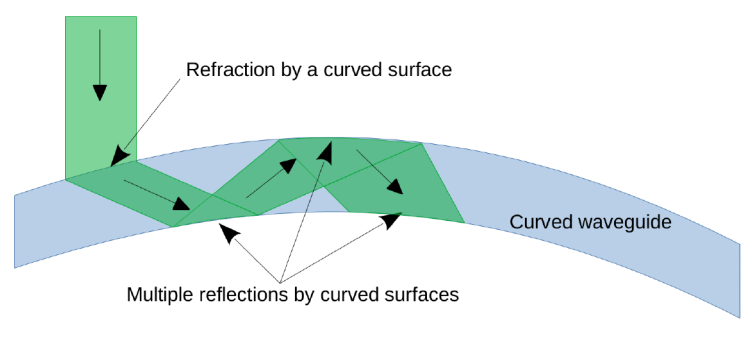

Fig. 1. Schematic of the light propagation in the curved waveguide and the different interactions with the curved surfaces susceptible to induced image aberrations.

In first approximation, we can see from Fig. 1, that the initial refraction when the beam is injected into the waveguide will act as a cylindrical lens with a focal distance of $F = r/(n-1)$, where r is the radius of curvature, and n the index of refraction. Each reflection on the curved surface during the propagation will act as cylindrical mirrors with $F = r/2$, with alternating signs (see green beam traced in Fig. 2(a)). In addition, because the light is incident to the

Optics EXPRESS

curved surface with an acute angle, the reflection will have a shorter focal length and generates astigmatism. The amount of astigmatism induced by a curved surface has been explored by [10] where the focal length of a curved mirror can be described by $F = r * cos(\theta)/2$, with θ the angle of incidence. This can be seen in Fig. 2(a) where the red beam incident at 54° does not have a single focal point. Of course, for a cylindrical mirror, the beam is unaffected (stays collimated) in the direction orthogonal to the plane of curvature. In any case, the image will suffer optical aberrations that need to be corrected.

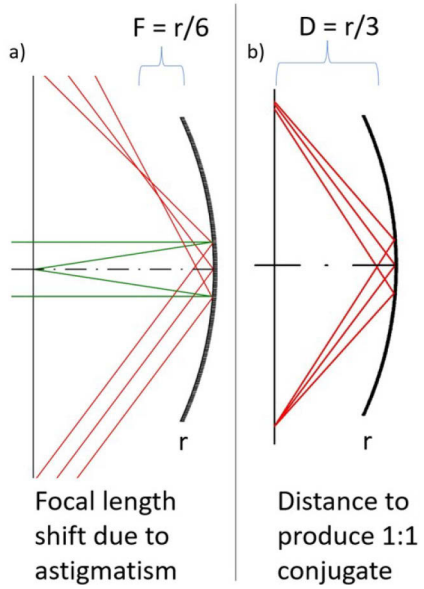

Fig. 2. a) shows a schematic showing the focal distance changing due to astigmatism for an off axis field of 54° in red, compared to the on axis focus in green. b) shows a 1:1 conjugate image plane can be seen if the source is positioned at a distance of $r/3$.

An important concept in previous waveguide head up display methods was that the light must propagate through the waveguide collimated so that the ray bundle does not expand or contract with distance [4]. This allowed for the extracted image to appear the same size across the eyebox. This concept applies to the curved waveguide as well where the image must stay the same size across the eye box. This cannot be accomplished with collimating the injection light, but there must be a constant focusing and expanding the ray bundle during propagation. The amount of focusing needed is dependent on the radius of curvature of the waveguide, the internal propagation angle, and is based on the amount of astigmatism the waveguide imparts on the light.

In order to correct the aberration, we first need to take into account the proper shape of the waveguide. A waveguide shape which preserves thickness is best suited for a curved waveguide. This shape is when the outer and inner radius of curvatures are concentric. It is important to note that this shape induces some residual power after each TIR bounce leading to astigmatism and defocus aberrations after long propagations through waveguides with relatively large thicknesses compared to radius of curvature. This happens from the radius of curvature being different between the 2 surfaces. In a cylindrically shaped waveguide, defocus only occurs in 1 direction while the other remains undisturbed. Modeling has shown that a waveguide with the same radius of curvature, but radially outward varying thickness produces undesirable aberrations beyond which a uniform thickness waveguide produces.

The H_{in} couples the light into the waveguide as well as applying the appropriate correction to the light. The H_{in} is recorded such that it allows the internally propagating ray bundle to

Optics EXPRESS

remain close to constant after each TIR bounce. A steeper or shallower center insertion angle will cause the scaling factor to be different. The thickness of the substrate and the size of the H_{in} are dependent on each other. A thicker substrate allows for a larger H_{in}. The equation, $\tan(\theta) = x/2t$, relates the central angle used for propagation (θ) and the size of the H_{in} (x) and the thickness of the substrate or waveguide (t). The size of the H_{in} is the initial pupil of the system and should match the exit pupil of the projector for efficient throughput and so the eye box has no spatial positions where the projected image cannot be viewed. If no expansion is used, then the pupil is virtual to the viewer and the entire field of view of the image cannot be seen. Only parts may be seen if the viewer moves their eye across the entire eye box. [10]

The focused light will be astigmatic where the tangential rays must focus at a distance of about $f_t = r/3$. This can be calculated by the previously mentioned equation for the astigmatic focal length of a curved mirror $F = r * cos(\theta)/2$, using theta = 54°. This relationship holds for any reflector curvature. At $r/3$, the 1:1 conjugate is satisfied for the off-axis rays. When the rays interact with the inner portion of the waveguide, they will see a negatively curved mirrored surface which will expand the ray bundles appropriately to allow for an overall unchanging image propagation method. It can be seen on the right side of Fig. 2 that, at a 54° angle of incidence, the astigmatism from a curved surface will change the focus to a factor of $\sim r/3$.

To propagate light internally of a curved waveguide, the light must undergo a balancing act between expanding and focusing as it interacts with the top and bottom surfaces through TIR. The summation of this through the waveguide allows for the H_{out}s to outcouple the light with little aberration. A spectrum can propagate through the waveguide since reflection is agnostic to wavelength. The main aberration the light undergoes as it TIRs in a 1D curved waveguide is compiling astigmatism as the light interacts with the front and back surfaces of the waveguide which have different power. At the centered angle of the propagating light through the waveguide, the rays must interact with the next surface as if it were a 1:1 imaging conjugate. Therefore, the H_{in} must have astigmatic power where the rays focus at this 1:1 conjugate location. The amount of power in the hologram to achieve this balancing act is shown in Fig. 3. Figure 4 shows a schematic of the focusing power the H_{in} must produce for a central propagation angle of 54° which should have a focus at $r/3$. The H_{in} should both induce this correction and couple the light into the waveguide for a more simple system.

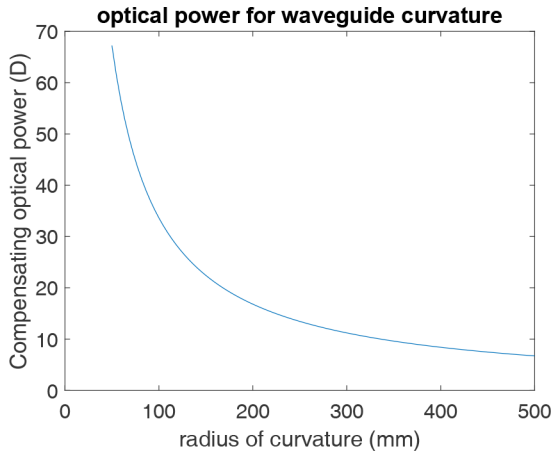

Fig. 3. H_{in} optical power required to induce a 1:1 conjugate continually propagating image through the waveguide based on the radius of curvature of the waveguide.

The H_{out} is segmented where each hologram is created with different geometry due to the waveguide curvature. This is to ensure that each section of the H_{out} outcouples the light parallel

Optics EXPRESS

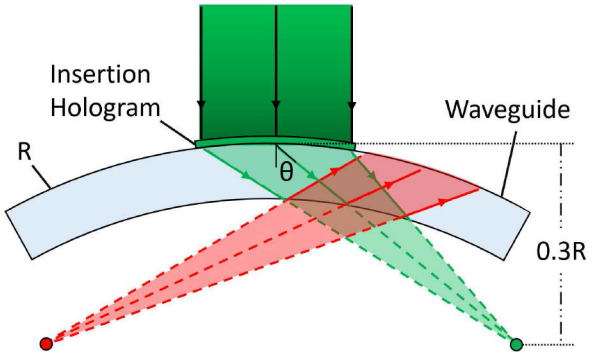

Fig. 4. H_{in} geometric correction showing the sagittal focus induced in green and the resulting virtual focus from the TIR off the waveguide surface in red.

across the expanded pupil. Each H_{out} compensates for the residual optical power allowing for the outcoupled image to be viewed with minimal image defects. The H_{out} segments should have varying diffraction efficiency to provide uniform illumination to the viewer across the expanded eyebox. Another image defect to consider is image duplication in the extracted image. This can occur when an off axis ray bundle interacts with 2 different H_{out} segments.

3. Computer simulation

An optical model was created in Optic Studio Zemax to define the parameters for curved waveguide propagation. Figure 5(a) shows the layout of the system where an object beam is collimated (by a paraxial lens on top of the H_{in}, that is not visible in the figure) and coupled into the waveguide at TIR conditions using a single HOE. After propagation internally in the waveguide for about 20 mm, the light interacts with the extraction HOEs where each section of the hologram has a varying efficiency to outcouple a constant luminance across the eyebox.

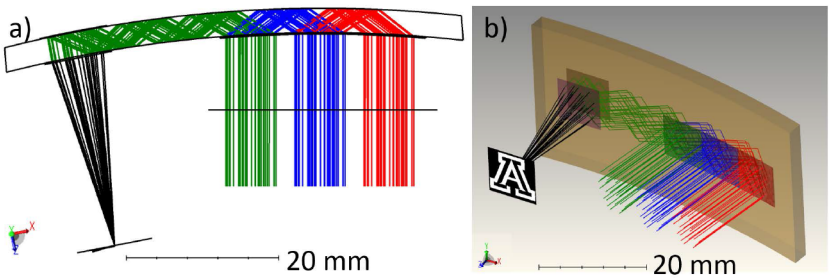

Fig. 5. a) is the top view of a 1-dimensional pupil expansion through a 1 dimensionally curved waveguide. The black rays show from the object to its collimating by a paraxial lens (not visible). The green rays represent the internally propagating light towards the 1^{st} H_{out} segment diffracted from the H_{in} located on the outer surface of the waveguide. The blue rays represent 2^{nd} pupil expansion and the red show the 3^{rd} expansion. b) is a 3D layout showing the projection optics, the curved waveguide, and each hologram section.

Figure 5(b) shows the ray tracing for a cylindrically curved waveguide (1D curvature) with an outer radius of curvature of 171.45 mm, thickness of 3.175 mm and an inner radius of curvature of 168 mm. The H_{in} is a 9 mm × 9 mm square. The H_{out} consists of 3 segments with a total size of 9 mm × 27 mm. The model is color coded where the black rays make up the projector, the green rays represent the internally propagating rays that are extracted at the 1^{st} segment. The blue

Optics EXPRESS

shows the rays which are not outcoupled at the 1st segment and continue to be outcoupled at the 2nd segment. The red rays show the 3rd segment extraction. Note that the model can demonstrate even more pupil replication segments as discussed later in the manuscript.

The H_{in} has added power of 8.06 D in the sagittal direction as well as the power introduced from being a curved surface with radius of curvature of 171.45 mm (2.879 D) and redirecting the light to propagate at a central angle of 54.6°. This angle can be varied slightly but should remain close to this value as it is between the angle for which the light does not TIR, or misses the H_{out}s. In our simulation, the materials had an index of 1.5, as index changes, the injection angle should be adjusted so that the fields of the image propagate through the waveguide without outcoupling. To obtain an efficient system, the pupil of the projection system should be located at the H_{in}. This ensures maximum insertion of the light in the waveguide and minimum footprint of the H_{in}.

The light then interacts with the inner and outer surface of the waveguide which are opposite in power. This implies that the astigmatism that each surface generates on the wavefront are of opposite sign. This allows for each field to propagation with minimal change in the ray bundle. The field of view is set by the index of refraction of the waveguide which allows for greater angular ranges as index of refraction is increased. Light is outcoupled if the angle of light does not satisfy TIR conditions or misses the H_{out} at the FOV extremes.

The H_{out} corrects any residual power and extracts the light out of the waveguide. The 1st H_{out} accepts the focusing light from the reflection of the outer surface and outcouples a portion of the light and focuses the light at a focal distance equal to the power of the curvature of the inner side of the waveguide. The inner curved surface will then collimate the light for the viewer to see in the far field. The remaining light continues bouncing and is extracted in the same manner by the remaining H_{out}s except for an angular difference. The extraction angle must be changed to compensate for the H_{out}s not being normal to the same plane as each other. The angle is equal to the angle change between the centers of each hologram when referenced to the center of curvature of the waveguide. The residual aberration could be described as the difference in aberration from the replicated pupils across the expanded pupil which leads to focus errors and image duplication. A summation of the hologram parameters for Optic Studio's Zemax non-sequential model can be seen in Table 1. Astigmatic power was added since the hologram lens feature in Zemax does not allow for differentiation of tangential and sagittal hologram creation terms.

In order to compare the image quality with or without correction in the injection HOE, the added power was removed in the ray trace model. The comparison between the outcoupled images across the eyebox can be seen in Fig. 6. Figure 6(a), the uncorrected H_{in} creates an image which has an image duplication effect as well as changes in focus across the field of view. Only the central portion of the image is focused at infinity. In Fig. 6(b), one can see that by using the corrected H_{in} the image is free from aberrations across the expanded pupil of 5.5 mm × 23.5 mm at 1 cm from the combiner and over a FOV of 30° × 30°. Two rays were propagated through the waveguide to show the difference between the uncorrected and corrected methods for a +4.5° field in Fig. 7. This ray trace shows 2 rays interacting with different portions of the entrance pupil of the waveguide combiner from the same point off-axis. The uncorrected propagation produces image duplication, and the duplicated points are out of focus. The corrected propagation method produces a single point free from aberration across the expanded pupil.

The corrected combiner field of view performance over 3 expanded pupils is shown in Fig. 8 using a spectrum of 20 nm centered at 532 nm. A grid of point sources was imaged through the curved waveguide to show off axis performance of this system. It can be seen that the imaged dots are best in the center FOV and lose clarity off axis. This is due to the compiling astigmatism from different fields interacting with the waveguide a different amount of times than the on axis ray bundle and from image duplication. If the off axis fields experience a different power from different number of interactions with the waveguide through TIR, the power induced in the different fields produces images at image depth locations other than at infinity. It has been seen

Optics EXPRESS

Table 1. The hologram parameters for the curved waveguide display system modeled in Optic Studio's Zemax non-sequential mode with 3x pupil expansion. The cylindrical waveguide has an outer radius of curvature of 171.45 mm and inner of 168.275 mm.

Hologram Parameters				
Hologram	Insert	1^{st} Ext	2^{nd} Ext	3^{rd} Ext
Type	Reflect	Trans	Trans	Trans
X_{ref} (mm)	−1.41E8	−1.5E8	−1.5E8	−1.5E8
Y_{ref} (mm)	0	0	0	0
Z_{ref} (mm)	−1E8	1E8	1E8	1E8
Tan add power (D)	8.06	0	0	0
Sag add power (D)	0	10	10	10
X_{obj} (mm)	0	5.297	0	−5.297
Y_{obj} (mm)	0	0	0	0
Z_{obj} (mm)	1E8	147.5	147.5	147.5
$\lambda_{rec}/n(\mu m)$	0.357	0.357	0.357	0.357
n	1.5	1.5	1.5	1.5
Efficiency %	100	33	50	100

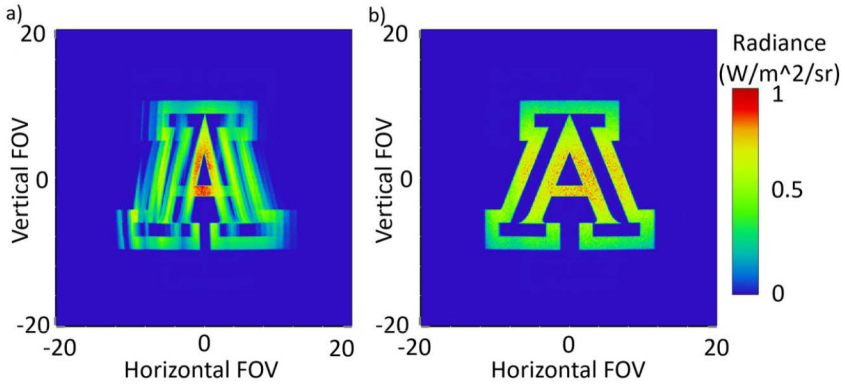

Fig. 6. Simulated image seen in radiance space through a waveguide at the expanded exit pupil without (a) and with (b) propagation correction.

Optics EXPRESS

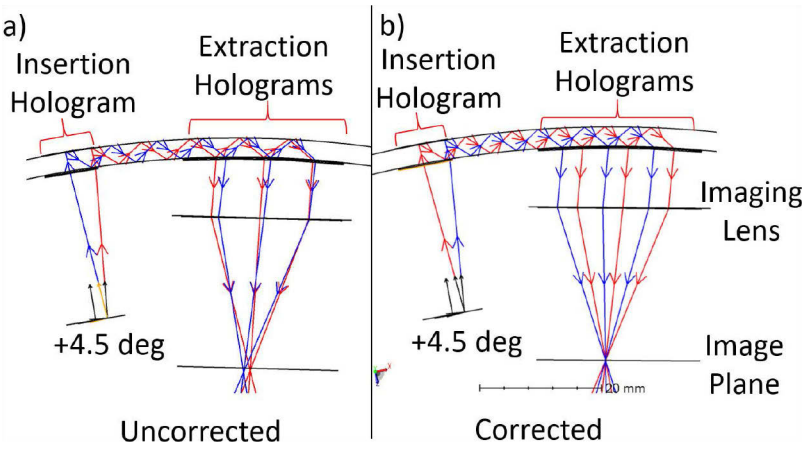

Fig. 7. Two ray propagation through a curved waveguide without (a) and with (b) propagation correction. Without propagation correction, an off axis point source creates 2 points which are out of focus. With propagation correction, a point source creates a single in focus image point.

in [4] that images produced at distances other than the focal length of the H_{out} can cause image duplication across an expanded pupil. Image duplication can occur if a ray bundle interacts with 2 or more different hologram segments resulting in a pointing error in the extracted rays producing 2 different images in angle space.

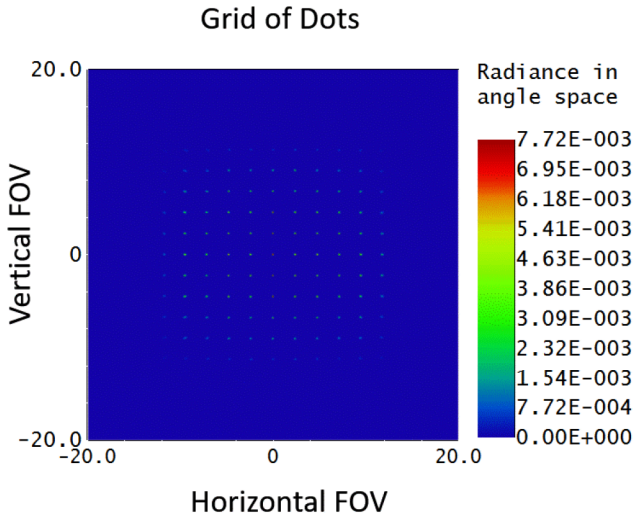

Fig. 8. The extracted image from a 3× pupil expansion was created by using a grid of point sources to show the performance over a wide field of view.

4. Demonstrator

A physical demonstrator of the simulated system was developed using a curved waveguide and HOEs laminated onto the waveguide surface. The waveguide was made from a commercially available 342.9 mm outer diameter acrylic tube. The thickness was 3.175 mm with an inner

Optics EXPRESS

radius of curvature of 168.275 mm. The HOEs consisted of an insertion and H_{out} which couples and corrects the TIR propagation within the waveguide and extracts the light toward the viewer.

The H_{in} was recorded in a transmission hologram geometry with a frequency doubled YAG coherent 532 nm laser. The hologram was recorded on Covestro Bayfol HX200 photopolymer which was laminated to the outer surface of the waveguide. A 25.4 mm right angle prism was index matched to the waveguide using an index matching oil and a plano-concave cylindrical lens. The radius of the cylindrical lens closely resembled the curvature of the waveguide. The object beam had astigmatic power where the focus was designed to be at 0.3×171.5 mm. This was accomplished by introducing an $f = 100$ mm cylindrical lens 34.3 mm from the right-angle prism hypotenuse face. The reference beam would be a collimated beam onto the curved surface of the waveguide. This required that the power of the reference beam would match the power of the curved waveguide outer surface. An astigmatic telescope was formed using 2 cylindrical lenses with $f = 100\ mm$ to achieve the appropriate power which matched the waveguide surface which was calculated to an effective focal length (f_w) of 351 mm. The reference beam was sent through the prism face which allows a total internal reflection to interact with the H_{in} at 0 degree incidence. This recording geometry allows for the use of the H_{in} without any extra lenses or coupling optics and can be seen in Fig. 9.

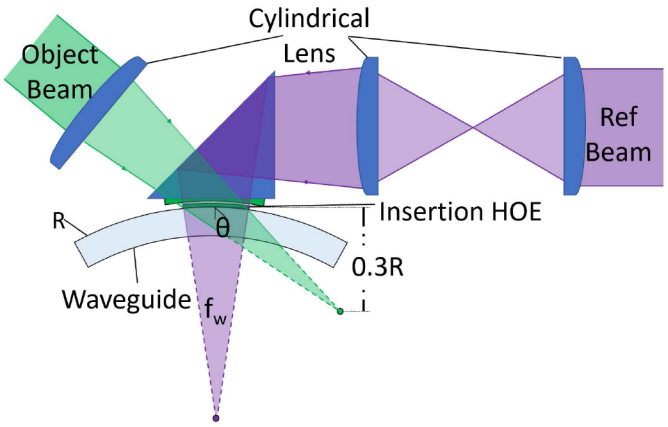

Fig. 9. Recording geometry for the insertion HOE showing the virtual focal points for the object and reference beams. The object beam focuses at $r/3$ from the waveguide outer surface while the reference beam focuses at the focal length of the waveguides outer surface for a 0 deg incidence angle. Cylindrical lenses are used in the recording to give the necessary power to the HOE.

The H_{out} was recorded in a reflection geometry with the photopolymer laminated to the outer surface of the waveguide. The H_{out} was recorded using a 532 nm writing laser beam coupled with the H_{in} as the reference beam. By coupling the reference beam with H_{in}, the entire H_{out} can be recorded all at once even though the reference beam is changing during its propagation into the waveguide. The object beam is a near collimated beam that covers the entire surface of the extraction zone, and which focal length sets the virtual image distance of the display (infinity in our case). The H_{out} recording geometry can be seen in Fig. 10.

Optics EXPRESS

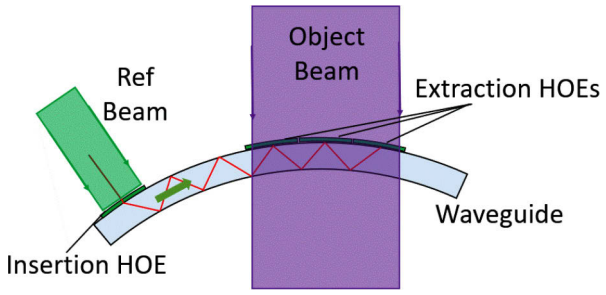

Fig. 10. Recording geometry for the extraction HOE showing the object and reference beams. The collimated reference beam is coupled by the H_{in} and propagates to the H_{out}. The reference beam is a collimated beam that cover the entire surface of H_{out} so the entire hologram is recorded all at once.

5. Results

The eyebox was expanded by 5 times in the horizontal direction through the curved waveguide. An image of an incident 532 nm laser beam on the H_{in} is coupled and extracted 5 times by an H_{out} is shown in Fig. 11. It is important to note that the extracted beams are parallel and collimated which are the conditions for a pupil replication projected at infinity without artifacts. It can also be noted that the extracted intensity decreases along the path of propagation since there is less and less light inside the waveguide after each extraction. To correct for this decreased intensity and offer a uniform image across the entire pupil, it is possible to modulate the diffraction efficiency of the H_{out}, starting with low efficiency and increasing it along the path of propagation. We already established the equation for the modulation in an earlier publication regarding planar waveguide. [3] Finally, the hazing of the waveguide that can be observed may be a result of poor waveguide surface quality causing diffuse surface scattering to be introduced into the hologram recording.

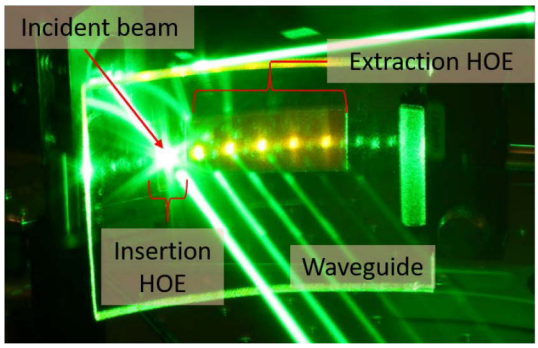

Fig. 11. Long exposure image of the curved combiner demonstrator extracting an incident 532 nm laser beam multiple times across the expanded pupil.

An amplitude chrome mask of a 1951 United States Air Force Resolution Target was imaged through the waveguide to determine the quality of image and was illuminated by a polychromatic source. It can be seen in Fig. 12(a) that group 3 element 3 of this target can be seen and corresponds to a resolution of the extracted image to be 18 cycles/deg. We calculated the modulation transfer function (MTF) curve using the picture of the target and the plot for both the horizontal and vertical direction is presented in Fig. 12(b).

Optics EXPRESS

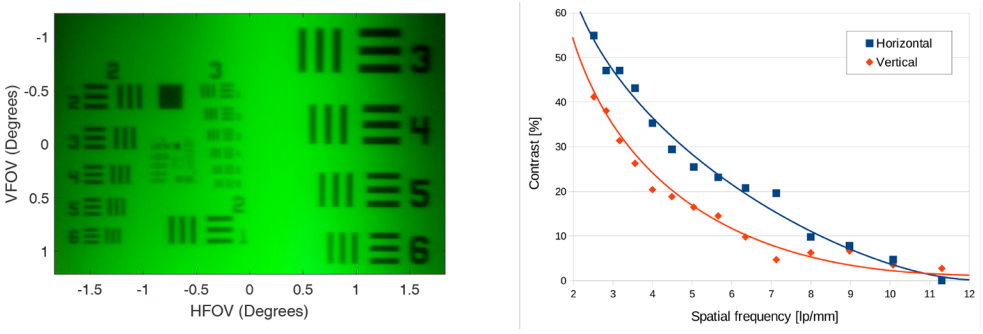

(a) Airforce resolution target picture (b) MTF graph

Fig. 12. Image resolution achieved through the curved waveguide: (a) Picture of a chrome mask Airforce resolution target showing that group 3 element 3 is still distinguishable with an angular resolution of 18 cycles/deg. (b) MTF plot calculated from the resolution chart picture, lines are guide for the eyes.

When measuring the FOV, it was seen that a polychromatic source expanded the FOV to a maximum of 13°(H) × 16°(V) with 532 nm accounting for the central angle over an expanded eyebox of 6.2 mm × 42.7 mm at 1 cm from the combiner. This FOV was measured by injecting a white uniform image in the waveguide and measuring the angular extend of the extracted image. If a large spectrum is used, the diffraction efficiency causes color non uniformity and can be difficult to obtain a stable white point for a full color system for a single waveguide, single hologram layer system. Some of that effect can be observed in Fig. 13 where the light from a LED picoprojector (3M MP180) is used as the source for the curved combiner. The picoprojector image is set to infinity, and the projector is placed as close as the injection hologram to capture a maximum of light since it has an internal pupil. Other than the aforementioned color shift, no other aberration was noticeable.

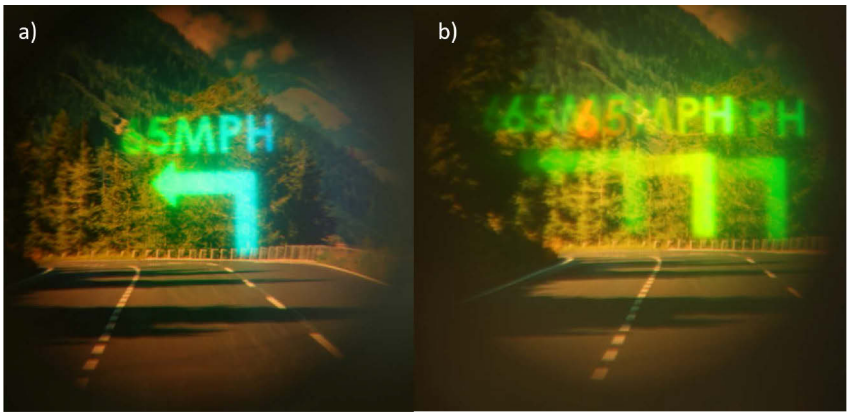

Fig. 13. a) shows the image is seen through the corrected waveguide while b) shows image duplication of 2.4 degrees seen through an uncorrected waveguide.

To test the effects of correction in the combiner a 2nd combiner was created which did not have the correction in the H_{in}. The H_{in} was a linear grating which would couple the light to TIR through the waveguide. The H_{out} was recorded in the same procedure as the corrected version using a single beam and the H_{in} producing the reference beam for the recording. The difference in extracted images is shown in Fig. 13 where the main aberration seen is image duplication in

Optics EXPRESS

the uncorrected combiner measured to have a difference of 2.4° between the images. This image duplication effect was also seen in the computer simulation when comparing the correction of the H_{in} to the uncorrected. The image was captured by overlaying the virtual information from the combiner with an image of a road which was near collimated by a lens so that they would be on the same image plane (i.e. infinity). This removes the need for accommodation between the virtually projected information from the curved combiner and the background. The arrow and text "65MPH" seen in Fig. 13 were projected by a pico projector which had its pupil relayed to the H_{in} of the curved combiner and has a polychromatic source. The color difference observed between the image seen through the corrected waveguide and seen through an uncorrected waveguide (Fig. 13 a and b) is due to the slight angle difference between the camera and the waveguide. Brightness and contrast differences are due to the automatic corrections operated by the camera software (Canon 50D DSLR). The 3 distinct replicated images seen in Fig. 13(b) are due to 3 consecutive extractions from the waveguide that are not parallel anymore. Each extraction that is entering the camera pupil is producing its own image in the angle space. A larger pupil size would present even more duplicated images. In Fig. 13(a), where the aberrations have been compensated for, the same 3 extraction overlaps, exactly as predicted by the model shown in Fig. 6 and Fig. 7.

For this demonstrator, degradation in the image as a function of pupil expansion was noticed and determined to come from the surface quality of the waveguide and holograms. The waveguide is a commercially available acrylic tube which has significant deviations in thickness as well as visible surface roughness leading to a highly scattering waveguide. The scattering affects the hologram recording processes which leads to degraded display quality as a function of internal TIR propagation.

6. Conclusion and future work

With propagation correction via HOEs, a curved waveguide with 1 dimensional pupil expansion can be used as a combiner. The light undergoes a combination of focusing and expansion through the waveguide which provides a quasi collimated state within the waveguide to allow for a minimally aberrated curved waveguide propagation and image extraction over an expanded pupil of 6.2 mm × 42.7 mm at 1 cm from the combiner.

It is possible to have greater image quality by using a curved waveguide which is manufactured to standard optical tolerances to have better thickness uniformity and surface quality.

The difference in power between the front and back surfaces of a waveguide puts a limit on how far light can propagate within a curved waveguide. As propagation distance increases, the negative power of the internal surface dominates the positive power from the outer surface but can be minimized by using thin waveguides because the inner and outer waveguide surfaces would have similar optical power. The H_{out} segments are recorded such that the power across the segments varies to extract a collimated image at each segment.

When the thickness of the waveguide decreases, the number of interactions with the surface increases which put a higher constrain on the surface quality. During ray tracing simulations, where waveguide surfaces without aberration were used, the proposed technique has shown no further limitation than the one due to the propagation distance. However, in real systems, it is to be expected that the thickness and surface irregularities of the waveguide will play an important role in the final image quality. Specifically, small scratches and other surface imperfection are creating stray light that reduces the image contrast. This is particularly visible in our prototype where the MTF value does not pass more than 55% (Fig. 12(b)). Indeed, the curved waveguide we used in this proof of concept was a cut off from an acrylic tube and has marginal optical properties. From the simulations as well as from our past experiences with high quality flat waveguides [3,11], it is expected that the stray light will be dramatically reduced when a curve waveguide with good optical surface quality (scratch and dig quality of 120/80 or lower) is used.

Optics EXPRESS

The waveguide relies on TIR which is wavelength agnostic, allowing for propagation of broadband sources as long as it satisfies the bragg conditions of the insertion and H_{out}s. The use of a polychromatic source is actually advantageous as it allows for a larger field of view in the combiner system. This effect can be seen in Fig. 13(a), where the source is a white light picoprojector. Because the diffraction angle depends of the wavelength (Bragg's law), the left part of the image has a longer wavelength (green) than the right part (blue). This color dispersion can be narrowed by using a thicker material for the HOEs, which will reduce their spectral bandwidth.

For color reproduction, red, green, and blue holograms can be used to have control over the spectra [12]. These holograms can be individually overlaid on the waveguide or multiplexed in the same material (if the material index modulation is large enough). The diffraction efficiency of the different HOEs should be carefully balanced to obtain a stable white point across the FOV of the extracted image.

The FOV can be extended further than the $13° \times 16°$ presented in this initial proof of concept which was limited by the bandwidth of the holographic material. The ray tracing model already demonstrated up to $30° \times 30°$ without aberration using ideal holograms. In addition, it is eventually possible to superpose two (or more) waveguides, each one carrying a complementary angular extend e.g.: $-30°$ to $0°$, and $0°$ to $+30°$, to achieve a very large FOV. Other techniques to increase further the FOV of waveguide combiners have also been published recently and can be applied to our system. [13,14]

Initial ray tracing simulations have shown it is possible to propagate through a 2 dimensionally curved waveguide such as a radially symmetric lens with the front and back surfaces being concentric seen in Fig. 14. 1-dimension pupil expansion through a 2D curved waveguide needs 2-dimensional correction in both the insertion and H_{out}s. The H_{in} needs a correction where the sagittal focus is at $r/3$ where r is the radius of curvature and now must include a tangential focus at r distance as described in Fig. 4. This allows for the light to focus and diverge in this other direction as it propagates by TIR through the waveguide.

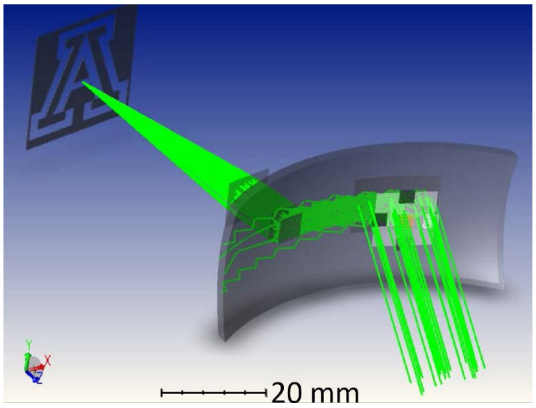

Fig. 14. Non sequential ray trace 3D layout of 1D pupil expansion through a 2D curved waveguide

Similarly, it is possible to extend this method to 2D expansion on 1D curved waveguide in an L-shaped configuration where a redirection hologram is required to redirect the horizontally light vertically for further pupil expansion. This can ultimately be extended to 2D pupil expansion within a 2D curved waveguide to allow for compact form factor systems which integrate well into HUD and NED systems.

Funding. Semiconductor Research Corporation (2810.052).

Optics EXPRESS

Acknowledgments. This work is supported in part by the Semiconductor Research Corporation Task No. 2810.052 through UT Dallas, Texas Analog Center of Excellence (TxACE), with Texas Instruments as primary sponsor and industrial liaison. I would like to thank my lab members and especially Luke Benoit for his helpful conversations during this work.

Disclosures. The authors declare no conflicts of interest.

Data availability. No data were generated or analyzed in the presented research.

References

1. B. C. Kress, "Optical waveguide combiners for AR headsets: features and limitations," in *Digital Optical Technologies 2019*, vol. 11062 B. C. Kress and P. Schelkens, eds., International Society for Optics and Photonics (SPIE, 2019), pp. 75–100.
2. C. Chang, K. Bang, G. Wetzstein, B. Lee, and L. Gao, "Toward the next-generation vr/ar optics: a review of holographic near-eye displays from a human-centric perspective," Optica **7**(11), 1563–1578 (2020).
3. C. T. Draper, C. M. Bigler, M. S. Mann, K. Sarma, and P.-A. Blanche, "Holographic waveguide head-up display with 2-d pupil expansion and longitudinal image magnification," Appl. Opt. **58**(5), A251–A257 (2019).
4. C. T. Draper and P.-A. Blanche, "Examining aberrations due to depth of field in holographic pupil replication waveguide systems," Appl. Opt. **60**(6), 1653–1659 (2021).
5. T. Levola, "Diffractive optics for virtual reality displays," J. Soc. Inf. Disp. **14**(5), 467–475 (2006).
6. B. C. Kress and I. Chatterjee, "Waveguide combiners for mixed reality headsets: a nanophotonics design perspective," Nanophotonics **10**(1), 41–74 (2020).
7. Y.-H. Lee, T. Zhan, and S.-T. Wu, "Prospects and challenges in augmented reality displays," Virtual Real. Intell. **1**(1), 10–20 (2019).
8. T. Zhan, Y.-H. Lee, G. Tan, J. Xiong, K. Yin, F. Gou, J. Zou, N. Zhang, D. Zhao, J. Yang, S. Liu, and S.-T. Wu, "Pancharatnam–berry optical elements for head-up and near-eye displays," J. Opt. Soc. Am. B **36**(5), D52–D65 (2019).
9. A. Kalinina and A. Putilin, "Wide-field-of-view augmented reality eyeglasses using curved wedge waveguide," in *Digital Optics for Immersive Displays II*, vol. 11350 B. C. Kress and C. Peroz, eds., International Society for Optics and Photonics (SPIE, 2020), pp. 27–34.
10. E. A. Igel and R. L. Hughes, "Optical analysis of solar facility heliostats," Sol. Energy **22**(3), 283–295 (1979).
11. C. M. Bigler, P.-A. Blanche, and K. Sarma, "Holographic waveguide heads-up display for longitudinal image magnification and pupil expansion," Appl. Opt. **57**(9), 2007–2013 (2018).
12. J.-A. Piao, G. Li, M.-L. Piao, and N. Kim, "Full color holographic optical element fabrication for waveguide-type head mounted display using photopolymer," J. Opt. Soc. Korea **17**(3), 242–248 (2013).
13. K. Yin, H.-Y. Lin, and S.-T. Wu, "Chirped polarization volume grating for wide fov and high-efficiency waveguide-based ar displays," J. Soc. Inf. Disp. **28**(4), 368–374 (2020).
14. J. Xiong, G. Tan, T. Zhan, and S.-T. Wu, "Breaking the field-of-view limit in augmented reality with a scanning waveguide display," OSA Continuum **3**(10), 2730–2740 (2020).